ISSN 0001-4338, Izvestiya, Atmospheric and Oceanic Physics, 2020, Vol. 56, No. 9, pp. 1053–1061. © Pleiades Publishing, Ltd., 2020.
Russian Text © The Author(s), 2019, published in Issledovanie Zemli iz Kosmosa, 2019, No. 5, pp. 3–14.

USE OF SPACE INFORMATION ABOUT THE EARTH STUDYING CATASTROPHIC NATURAL PROCESSES FROM SPACE

Monitoring Landslide Processes by Means of L-Band Radar Interferometric Observations: Using the Example of the Bureya River Bank Caving

V. G. Bondur[a, *], L. N. Zakharova[b], A. I. Zakharov[b, **], T. N. Chimitdorzhiev[c, *], A. V. Dmitriev[c], and P. N. Dagurov[c]**

[a] *AEROCOSMOS Research Institute for Aerospace Monitoring, Moscow, Russia*
[b] *Kotelnikov Institute of Radioengineering and Electronics, Russian Academy of Sciences, Fryazino Branch, Fryazino, Russia*
[c] *Institute of Physical Materials Science, Siberian Branch, Russian Academy of Sciences, Ulan-Ude, Russia*
**e-mail: vgbondur@aerocosmos.info*
***e-mail: ludmila@sunclass.ire.rssi.ru*
****e-mail: tchimit@gmail.com*

Received September 4, 2019; revised September 6, 2019; accepted September 9, 2019

Abstract—The possibilities of interferometric surveying using L-band PALSAR-1 and PALSAR-2 space radars on the ALOS-1 and ALOS-2 satellites for studying landslide processes are analyzed using the example of a catastrophic caving of ~18.5 million m^3 on the Bureya River in December 2018. The motions of the landslide surface are revealed and their integral amplitude is estimated at time intervals of up to 2 years. It is found that summer images are less informative due to a dramatic loss of coherence due to heavy rainfall; almost all winter pairs of images taken at low negative temperatures have high coherence due to the stability of the dielectric properties of wood vegetation and underlying soils. Based on the analysis of the dynamics of the development of the landslide process over a 10-year time interval, it is shown that soil displacements along the slope were small in 2006–2010 (1.6–1.9 cm/month); in 2015–2016, the displacements increased significantly (4.7–4.9 cm/month), and the maximum measured velocity of displacements was reached in the summer of 2016 (10.7 cm/month). It has been suggested that intensification of the landslide process occurred at the time the filling of the reservoir basin was completed in 2006–2009; the process was triggered by both the initial rise and seasonal fluctuations in water levels.

Keywords: Earth remote sensing, synthetic aperture radar (SAR), SAR images, SAR interferometry, surface displacement, landslide, Bureya River

DOI: 10.1134/S0001433820090078

INTRODUCTION

Recently, there has been an increase in the number of natural disasters and the negative consequences they cause (Bondur et al., 2009, 2012; Natural Hazards, 2000). Hence, new methods and technologies for monitoring and predicting hazardous natural processes are being developed, including earthquakes (Akopyan et al., 2017; Bondur and Zverev, 2005, 2007; Bondur et al., 2007, 2010, 2016a, 2016b; Bondur and Smirnov, 2005), typhoons (Bondur et al., 2008a, 2008b; 2009, 2012), landslides (Zakharova et al., 2019; Kramareva et al., 2018, 2019; Bondur et al., 2019a, 2019b), mudflows, avalanches, etc. (*Prirodnye opasnosti*..., 2000; Bondur et al., 2009, 2012). Methods and means of Earth remote sensing (ERS) and, first of all, all-weather radar methods play an important role in solving these problems (Verba et al., 2010; Bondur et al., 2009, 2019a, 2019b, 2019c; Bondur, 2010; Bondur and Chimitdorzhiev, 2008a, 2008b; Zakharova et al., 2019; Zakharov and Zakharova, 2017; Zakharova and Zakharov, 2019), as well as methods for processing aerospace images (Bondur and Starchenkov, 2001).

SAR interferometry methods as a tool for detecting small-scale displacements of the underlying surface (Bamler and Hartl, 1998) have been used for a long time in Earth remote sensing. Examples of the application of SAR interferometry methods include monitoring landslide activity (Kimura et al., 2000; Colesanti et al., 2006; Bondur et al., 2019a, 2019b; Zakharova, 2019; Zakharova et al., 2019; Zakharova and Zakharov, 2019), cryogenic soil deformations (Chimitdorzhiev et al., 2011), and soil subsidence due to economic activities (Strozzi et al., 2003; Epov et al., 2012).

In this paper, we consider the possibilities of using interferometric methods for monitoring landslide processes using the example of the collapse of the slope of

the Bureya River, which occurred on December 11, 2018. We used the classical method of differential SAR interferometry.

OBJECT OF RESEARCH AND THE DATA AND PECULIARITIES OF DATA PROCESSING

The catastrophic landslide on the landslide slope of the Bureya River, which occurred on December 11, 2018, attracted much attention from specialists and researchers (Kramareva et al., 2018, 2019; Zakharova et al., 2019; Bondur et al. 2019a, 2019b). The length of the sliding surface of the landslide was about 800 m, the width was about 400 m, and the volume of the removed ground was 18.5–18.9 million m^3 (Ostroukhov, 2019). The main unresolved issue is finding out the causes of the landslide and the time ground motions began.

The Bureya is one of the most abundant tributaries of the Amur River. In the upper reaches, the velocity of this mountain river is 3–4 m/s. In the middle part, the river crosses the spurs of the Bureinsky and Turana ridges and flows along a narrow canyonlike valley. In the lower part it flows out onto the Zeya-Bureinsky Plain. The river is fed with mixed monsoon floods. Before the creation of the Bureya Reservoir, floods occurred here almost every year, and catastrophic floods occurred once every 10 years (Korenyuk, 2009). The narrow canyon river bed in the landslide area is the middle part of the 230-km reservoir. As a result of the rise in water level as the reservoir was filled, the width of the river here increased from 200 to 400 m, and the channel of the Srednyi Sandar stream, which flows into the Bureya opposite to the place of the landslide, was flooded 1.6 km upstream. Based on the SRTM and TanDEM-X digital elevation models, the water level at the mouth of the stream increased by at least 60 m. Since the river section in the landslide area is part of the reservoir, seasonal fluctuations in the water level near the dam with a height of about 16–19 m are observed here. They are the cause of deforestation in a narrow coastal strip on the coastal slopes and, probably, the cause of the development of landslide processes (Ostroukhov et al., 2019). The climate in this region is sharply continental, with temperatures of 28°C in summer and –25°C in winter. The wettest month of the year is July, with 10 rainy days and a monthly rainfall reaching 140 mm.

The efficiency of the use of interferometric observations of the Earth's surface from repeated satellite orbits depends on the type of underlying surface and weather conditions in the survey areas. One essential feature of the surrounding area in the middle canyon part of the Bureya River bed with the landslide area is the presence of a developed vegetation layer, larch forests. On the northern slopes, the forest floor is covered with green moss and, on the southern slopes, they have a herb layer. Since the landslide slope was covered with forest vegetation, this made it difficult to find permanent scatterers (Bondur et al., 2019; Bondur and Chimitdorzhiev, 2008a, 2008b). At the same time, under certain weather conditions, the forest aggregate with the underlying surface can be used for interferometric analysis as an extended target.

It is noteworthy that the temporal decorrelation of the backscattered signals obtained in two different observations often leads to strong noise in the phase difference in the interferogram, which makes the measurements unreliable. The permanent scatterers method solves the problem of temporal decorrelation by identifying natural scatterers (Ferretti et al., 2000). Permanent scatterers, the pointlike bright radar targets, give stable reflection in both amplitude and phase. They are identified by the statistical analysis of data generated using a long series of repeated radar observations of a selected surface region. As a result, it is possible to carry out phase measurements even in the case of the complete loss of correlation of the signals of the surrounding natural landcovers.

Promising versions of the permanent scatterers method include the StaMPS method (Stanford Method for Persistent Scatterers) (Hooper et al., 2007), the SqueeSAR method (Ferretti et al., 2011), and the small baseline method (Bernardino et al., 2002). In addition to the natural scatterers, artificial stable targets are often used to reveal the dynamics of the underlying surface, for example, corner reflectors (Strozzi et al., 2013; Fu et al., 2010; Xia et al., 2004).

The first studies of the Bureya landslide by the interferometric method were carried out using the data from the European C-band synthetic aperture radar installed on the Sentinel-1 satellite. The beginning of surveys of this region from this satellite falls on the summer of 2016 (Zakharova and Zakharov, 2019). Such surveys showed that, in the winter of 2016–2017, vertical displacements of soils on the coastal slope of about 3.5 cm per month were observed in the direction downslope. The observation of soil motions on a slope covered with woody vegetation on radar images from the Sentinel-1 satellite in the autumn and spring period, as well as in summer, turned out to be impossible due to the high temporal decorrelation of echoes of this radar, which has a wavelength of 5.6 cm.

L-band radars are more suitable tools whose data are more robust to temporal decorrelation. The images used in this work obtained using the Japanese PALSAR-1 radar (wavelength 24 cm) of the ALOS-1 satellite have been available for analysis since the summer of 2006, when the reservoir was still being filled with water until March 2011. Radar images from the PALSAR-2 radar (wavelength also 24 cm) installed on board the ALOS-2 satellite have been used since autumn 2014 at the time of preparation of this paper.

ALOS-1 satellite's orbit repetition cycle is equal to 46 days; thus, it is possible to obtain interferometric pairs, the interval between which is a multiple of 46 days. Due to the drift of orbital parameters and rare

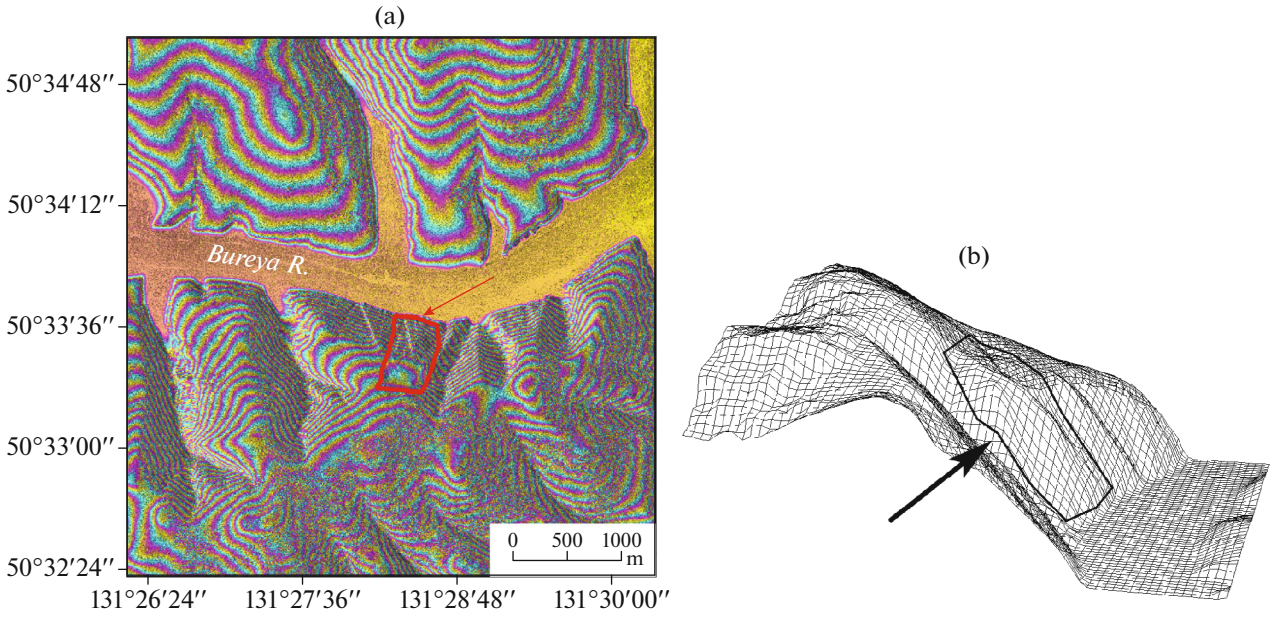

Fig. 1. Fragment of the interferometric phase difference of the radar echo signals of the TerraSAR-X/TanDEM-X satellites (a) and three-dimensional visualization of the digital model of the landslide slope topography (b).

but significant orbital corrections, the interferometric base changed within 0–20 km over 2 years of operation of this satellite.

The interval of repeated (interferometric) imagery from the ALOS-2 satellite is a multiple of 14 days. Due to frequent small corrections of the orbit of the ALOS-2 satellite, the interferometric baseline stayed within in a tube with a diameter of 500 m.

Radar data processing was carried out using the ENVI SARScape software package with differential radar interferometry technique. It consists in the estimation of the phase component on the interferogram due to the displacement of the target. TerraSAR-X/TanDEM-X digital elevation model (DEM) with 5 m resolution acquired in April 2012 was used for subtraction of topographic phase.

Figure 1a shows a fragment of the TerraSAR-X/TanDEM-X interferogram, which characterizes the terrain. This and some other results are duplicated on the web page (*Opolzen*..., 2019). Repeating color cycles in the interferogram (interferometric fringes in the Fig. 1a) correspond to phase values registered by radar modulo 2π.

A change in the signal phase difference by 2π (one color cycle in Fig. 1a) in the geometry of the imagery from the TerraSAR-X satellite corresponds to a change in the terrain topography height by 16.7 m. The contour of the collapse zone in December 2018 (closed red line) is indicated by an arrow in Fig. 1a. The 3D representation of the digital elevation model before the collapse is shown in Fig. 1b, where the arrow also indicates the contour of the collapse zone.

Archives of the Japan Aerospace Exploration Agency (JAXA) contain 32 radar images of the landslide area made by the PALSAR-1 radar of the ALOS-1 satellite from tracks 414, 415, 418, and 419, as well as 16 images from the PALSAR-2 radar of the ALOS-2 satellite from tracks 127 and 128, which are suitable for interferometric processing.

The coherence of signals from an interferometric pair is an important indicator of the quality of interferometric measurements. The coherence depends primarily on the length of the perpendicular component of the interferometric baseline, the time interval between the acquisition of a pair of images, and the weather conditions on the days of imaging and the day before. Temporal decorrelation of the backscattered signals indicates changes in scattering properties of the target as an effect of nonsimultaneous observations.

Due to the relatively long wavelength of the PALSAR-1 and PALSAR-2 radars, the temporal stability of backscatter is higher than that of the C-band radars. As a result, it is possible, for example, to obtain quite informative interferometric pairs with an interval between surveys of up to 2 years using the radar images in the winter season. However, summer radar images are less suitable for measurements due to the significant temporal decorrelation of radar echoes caused by heavy rains shortly before or during the survey.

The source of information on air temperature and precipitation was the data from the Sektagli meteorological station located 35 km west of the landslide site (www.rp5.ru).

Archive radar images have been carefully analyzed for selecting the interferometric pairs. First, they were

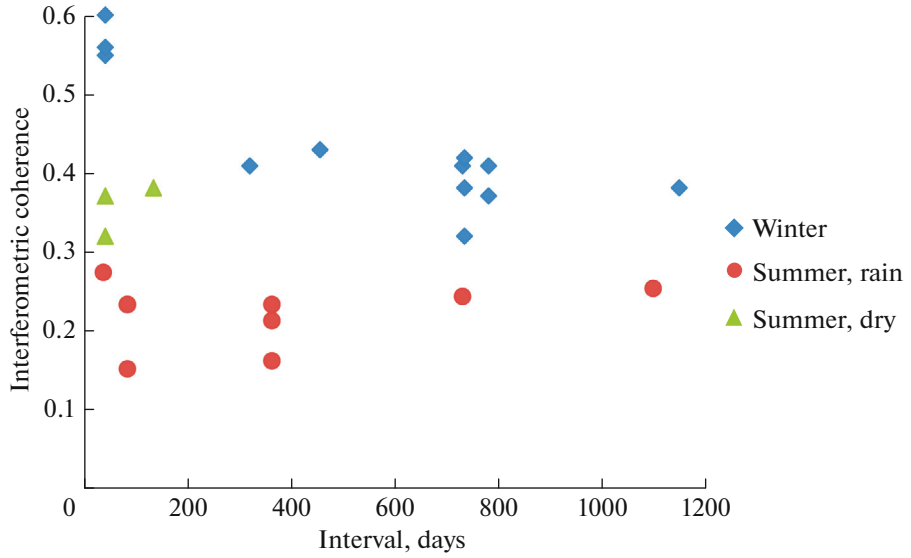

Fig. 2. Coherence of the ALOS-1 PALSAR-1 signals (vertical axis) depending on the interval between surveys of the interferometric pair (horizontal axis, days).

divided into winter and summer ones. Winter images were radar images at negative average air temperatures for 3 days, including the day of imaging. Winter and summer radar images were not combined into interferometric pairs due to the strongly changing dielectric properties of the scattering surface during freezing, which leads to a severe decrease in coherence. In addition, pairs of images with interferometric baseline greater than 4 km were excluded from consideration.

Figure 2 shows the interferometric coherence for 23 pairs of radar images of the landslide zone from the PALSAR-1 radar of the ALOS-1 satellite. One can see that the highest coherence is observed in the pairs of images taken in the cold season (diamond-shaped markers). In this case, as the interval between the acquisition of a pair of radar images increases, the coherence is expected to decrease. Quite a high coherence was observed between several pairs of images in dry weather in summer (triangles). Rainy weather on the days of the survey or on the days preceding the survey, with a total amount of precipitation for 4 days prior to the survey exceeding 20 mm, led to a strong drop in coherence (round markers) and loss of information content of phase measurements. The results of measurements of the Earth's surface displacements described below were obtained by analyzing pairs of images with coherence above 0.3.

Figure 3 illustrates similar measurements of the PALSAR-2 radar from ALOS-2. Only three pairs of summer images (triangles in Fig. 3) out of 19 pairs of radar images from this satellite have a sufficiently high coherence (exceeding 0.3). The coherence from most summer pairs of radar images (circles in Fig. 3) is below 0.3 due to rainy weather; the total amount of precipitation exceeds 25 mm during the 4 days preceding the survey; they are not informative. All pairs of winter radar images from the ALOS-2 satellite (diamonds in Fig. 3) are characterized by low coherence due to the absence of frost on the days of the survey (the temperature was about 0°C), which may have caused repeated thawing–freezing of the upper layer of the scattering surface.

PROCESSING RESULTS AND THEIR ANALYSIS

After processing the selected 42 pairs of radar images and analyzing the results, only 12 interferograms were recognized as informative in accordance with the levels of coherence mentioned above.

Figure 4a shows the summer differential interferogram based on the data from the ALOS-2 satellite, with an interval between surveys of 28 days (June 15, 2016– July 13, 2016). A noisy strip of the river with three large northern tributaries and one southern tributary stands out brightly over the dark background of the land. The landslide zone located on the opposite bank of the mouth of the Sredny Sandar stream is clearly visible as an elongated light spot in comparison with the surrounding darker background (highlighted by enclosing it in a white ring). In the accepted processing scheme, the displacement of the reflecting surface away from the radar during the time between surveys leads to an increase in the phase difference, which is displayed in light tones on the interferogram. The uneven brightness of the spot indicates a higher speed of motion in the upper part of the landslide near the future separation wall. In this interferogram, the radial velocity of surface displacement changes within the landslide zone from 2 to 4 cm in 28 days, which, in

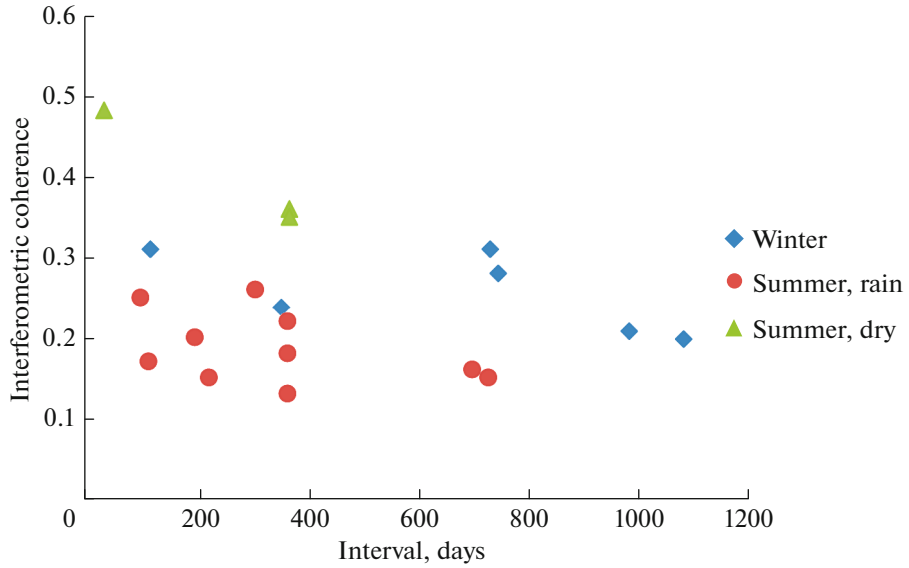

Fig. 3. Coherence of the ALOS-2 PALSAR-2 signals (vertical axis) depending on the interval between surveys of the interferometric pair (horizontal axis, days).

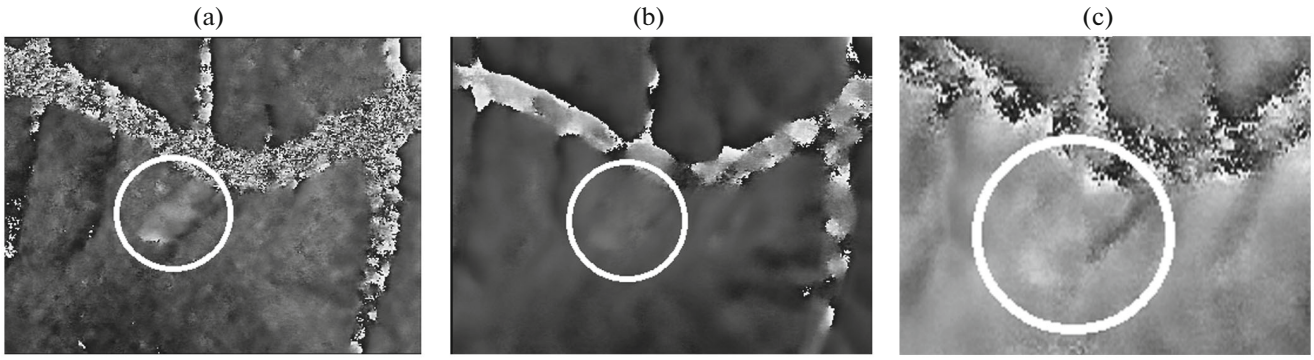

Fig. 4. Fragments of interferograms: ALOS-2 PALSAR-2 on June 15, 2016–July 13, 2016 (a); ALOS-1 PALSAR-1 on January 13, 2009–February 28, 2009 (b); ALOS-1 PALSAR-1 on May 16, 2006–October 1, 2006 (c).

terms of the displacement along the slope, gives up to 10.7 cm/month. This is vastly greater than 6 months later in winter from the Sentinel-1 data: 0.6 cm in 12 days, i.e., 3.4 cm/month on the slope (Zakharova and Zakharov, 2019).

An analysis of radar images from the ALOS-1 satellite in 2006–2010 shows that the phase drift due to shifts in the winter interferograms is not as large even with a greater interval between surveys than in summer 2016. This can be explained both by the earlier and slower stage of the development of the landslide process and by the greater stability of the frozen soil in the cold season. Figure 4b shows an interferogram January 13, 2009–February 28, 2009, in which the maximum phase difference on the landslide body with the average surrounding background is 0.6 radians, which corresponds to a radial displacement of less than 1.2 cm in 46 days (1.8 cm/month along the slope). On the summer interferogram May 16, 2006–October 1, 2006, based on the PALSAR-1 data (Fig. 4b), there is radial displacement with an amplitude of up to 2 cm in 92 days (1.6 cm/month along the slope), which is seen slightly better; it is six times smaller than the maximum displacement rate in the summer of 2016.

The effect accumulated over an interval of about a year or more is much more noticeable. Figure 5a shows an interferogram for a pair of radar images January 8, 2007–February 28, 2009. Here, the displacements of the Earth's surface in the upper part of the landslide are such that a phase wrapping takes place; in the interferogram in the landslide area, unlike in Fig. 4, a line of transition over 2π appears: a sharp border between black and white. In the lower part of the landslide, the radial displacement is about 8 cm; in the

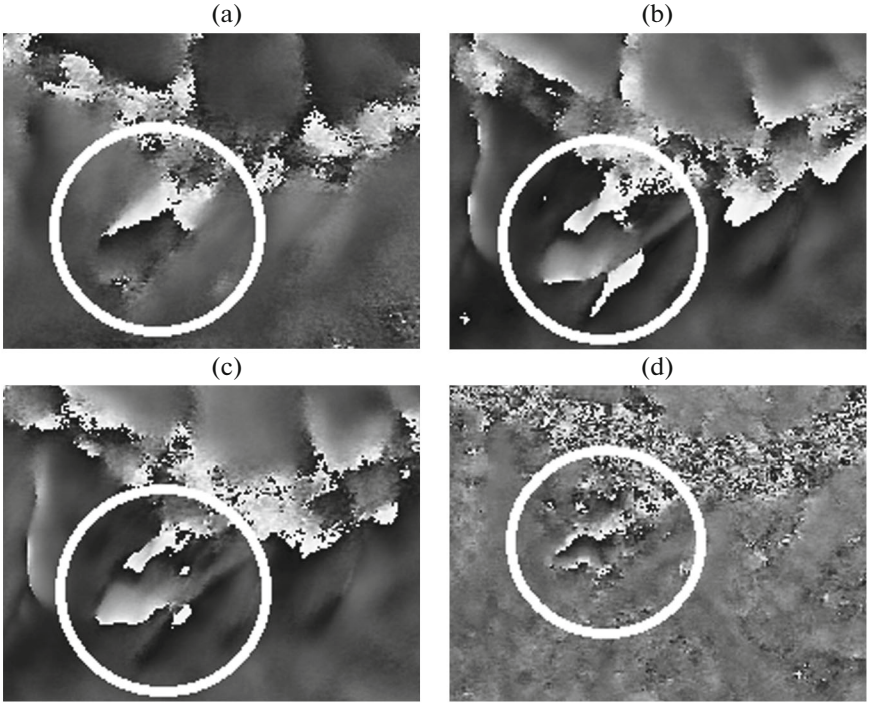

Fig. 5. Fragments of interferograms: on January 8, 2007–February 28, 2009 (a); on January 11, 2008–January 16, 2010 (b); on February 26, 2008–March 3, 2010 (c); and with a 1-year interval from June 22, 2015–June 20, 2016 (d).

upper part it is 14 cm in 2 years. The maximum velocity along the slope is 1.3 cm/month.

Surface displacement rates close to the last-mentioned ones were found in 2-year pairs January 11, 2008–January 16, 2010, and February 26, 2008–March 3, 2010; their interferograms are shown in Figs. 5b and 5c (1.5 and 1.9 cm/month down the slope). One peculiarity of these two interferograms is the presence of a significant snow cover of varying thickness on different observation days. According to the Sektagli meteorological station, the increase in the thickness of the snow cover between observations of the first pair was 8 cm; the difference in the second pair was 17 cm. It is known that the presence of a layer of fresh snow (about 6-cm-thick) that fell during the time between surveys leads to an increase in the signal path length by 1 cm (Zakharov and Zakharova, 2017). In this case, a homogeneous snow layer on the surface of a riverbank slope about 30–40 cm, as well as its increment during the time between surveys, almost did not affect the phase pattern in the interferograms, adding an unknown component to the phase difference, which is almost constant over the image.

According to the results of processing the interferometric pair June 22, 2015–June 20, 2016, of the PALSAR-2 radar (Fig. 5d), the maximum radial velocity of the Earth's surface displacement in 2016 reached 23 cm per year in the upper part of the landslide (4.7 cm/month down the slope). The pair in which each image was taken a month later, July 15, 2015–July 13, 2016, gives a close value of the displacement rate: 4.9 cm/month.

Figure 6 shows the maximum displacements for all mentioned pairs of the SAR data measured by subtracting the phase difference in the landslide area from the phase of the surrounding stationary regions on the corresponding interferograms, in terms of the displacement along the landslide slope for 30 days. The differences between displacement velocities in pairs from the PALSAR-1 radar in 2006–2010 over the intervals from 46 to 782 days are low and almost constant. The values estimated from the PALSAR-2 data in 2015–2016 are noticeably higher. The maximum velocity was observed in the summer of 2016; it exceeded 10 cm/month and approached those from the Sentinel-1 data at the beginning of winter 2017–2018: 7 cm in 12 days, or 17 cm/month down the slope (Zakharova and Zakharov, 2019).

The results indicate that the velocity of landslide motion in summer is usually higher than in winter. The lowest measured velocity of motion was noted in the beginning of the observation period in 2006.

The likely cause of the landslide process is filling of the reservoir (whose operating water level was reached in 2009) and the subsequent seasonal fluctuations in the water level. The maximum radial displacement (23 cm per year) was revealed at the end of the obser-

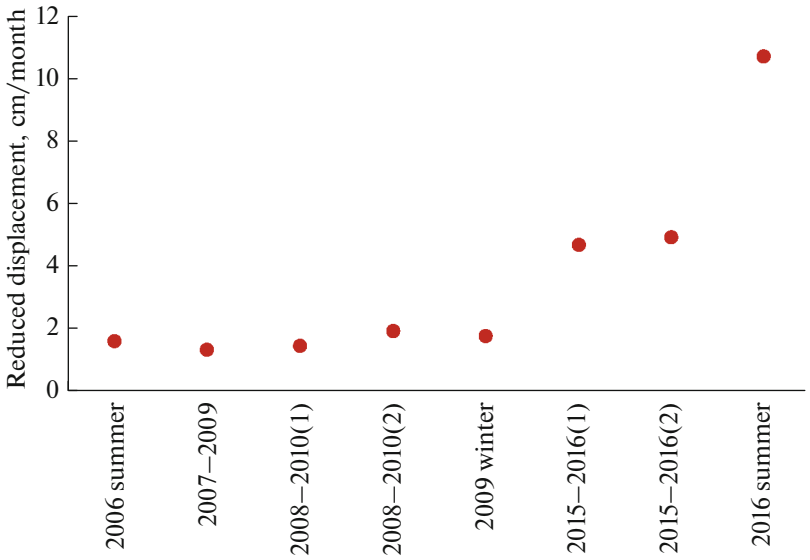

Fig. 6. Displacements measured on the interferograms of the PALSAR-1 (2006–2010) and PALSAR-2 (2015–2016) radars, reduced to cm/month down the slope.

vation period using the PALSAR-2 data taken not long before the landslide event.

CONCLUSIONS

Long-term monitoring of the landslide on the Bureya River over a 10-year time interval became possible due to the use of archived radar images from comparatively longwave L-band radars in 2006–2016. The scattering surface demonstrates high scattering stability in this frequency band, which allows obtaining integral estimates of surface motions over an interval of up to 2 years.

At the same time, summer radar images were often less informative due to a dramatic loss of coherence due to the heavy rainfall on the day of imaging or immediately before it. Almost all winter pairs of radar images taken at low negative temperatures had high coherence due to the high stability of the dielectric properties of woody vegetation and underlying soils.

The results of the research indicate the high efficiency of SAR interferometric methods of remote sensing for researching and monitoring dangerous natural processes such as landslides.

ACKNOWLEDGMENTS

We are grateful to JAXA for the ALOS PALSAR and ALOS-2 PALSAR-2 radar data provided as part of the RA-6 scientific projects and to the German Aerospace Center (DLR) for the TerraSAR X/TanDEM X data.

FUNDING

These studies were carried out as part of the state assignments of the AEROCOSMOS Research Institute for Aerospace Monitoring no. 075-00896-19-01 (theme no. ON58-2019-0030), the Kotelnikov Institute of Radioengineering and Electronics of the Russian Academy of Sciences, Institute of Physical Materials Science, Siberian Branch, Russian Academy of Science, and with support in part from the Russian Foundation for Basic Research (grant no. 18-07-00816).

REFERENCES

Akopian, S.Ts., Bondur, V.G., and Rogozhin, E.A., Technology for monitoring and forecasting strong earthquakes in Russia with the use of the seismic entropy method, *Izv., Phys. Solid Earth,* 2017, vol. 53, no. 1, pp. 32–51. https://doi.org/10.1134/S1069351317010025

Bamler, R. and Hartl, P., Synthetic aperture radar interferometry, *Inverse Probl.,* 1998, vol. 14.

Berardino, P., Fornaro, G., Lanari, R., and Sansosti, E., A new algorithm for surface deformation monitoring based on small baseline differential SAR interferograms, *IEEE Trans. Geosci. Remote Sens.,* 2002, vol. 40, no. 11, pp. 2375–2383.

Bondur, V.G., Zakharova, L.N., Zakharov, A.I., Chimitdorzhiev, T.N., Dmitriev, A.V., and Dagurov, P.N., Long-term monitoring of the landslide process on Bureya riverbank based on interferometric L-band radar data, *Sovr. Probl. Dist. Zond. Zemli Kosm.*, 2019a, vol. 16, no. 5, pp. 113–119. https://doi.org/10.21046/2070-7401-2019-16-5-113-119

Bondur, V.G. and Starchenkov, S.A., Methods and programs for aerospace imagery processing and classification, *Izv. Vyssh. Uchebn. Zaved., Geod. Aerofotos'emka,* 2001, no. 3, pp. 118–143.

Bondur, V.G. and Smirnov, V.M., Method for monitoring seismically hazardous territories by ionospheric varia-

tions recorded by satellite navigation systems, *Dokl., Earth Sci.,* 2005, vol. 403, no. 5, pp. 736–740.

Bondur, V.G. and Zverev, A.T., A method of earthquake forecast based on the lineament analysis of satellite images, *Dokl., Earth Sci.,* 2005, vol. 402, no. 4, pp. 561–567.

Bondur, V.G., Garagash, I.A., Gokhberg, M.B., Lapshin, V.M., Nechaev, Yu.V., Steblov, G.M., and Shalimov, S.L., Geomechanical models and ionospheric variations related to strongest earthquakes and weak influence of atmospheric pressure gradients, *Dokl., Earth Sci.,* 2007, vol. 414, no. 4, pp. 666–669.

Bondur, V.G. and Zverev, A.T., Lineament system formation mechanisms registered in space images during the monitoring of seismic danger areas, *Issled. Zemli Kosmosa,* 2007, no. 1, pp. 47–56.

Bondur, V.G., Pulinets, S.A., and Kim, G.A., Role of variations in galactic cosmic rays in tropical cyclogenesis: evidence of Hurricane Katrina, *Dokl., Earth Sci.,* 2008a, vol. 422, no. 7, pp. 1124–1128. https://doi.org/10.1134/S1028334X08070283

Bondur, V.G., Pulinets, S.A., and Uzunov, D., Ionospheric effect of large-scale atmospheric vortex by the example of hurricane Katrina, *Issled. Zemli Kosmosa,* 2008b, no. 6, pp. 3–11.

Bondur, V.G. and Chimitdorzhiev, T.N., Texture analysis of radar images of vegetation, *Izv. Vyssh. Uchebn. Zaved., Geod. Aerofotos'emka,* 2008a, no. 5, pp. 9–14.

Bondur, V.G. and Chimitdorzhiev, T.N., Remote sensing of vegetation by optical microwave methods, *Izv. Vyssh. Uchebn. Zaved., Geod. Aerofotos'emka,* 2008b, no. 6, pp. 64–73.

Bondur, V.G., Krapivin, V.F., and Savinykh, *V.P., Monitoring i prognozirovanie prirodnykh katastrof* (Monitoring and Forecasting of Natural Disasters), Moscow: Nauchnyi mir, 2009.

Bondur, V.G., Garagash, I.A., Gokhberg, M.B., Lapshin, V.M., and Nechaev, Yu.V., Connection between variations of the stress-strain state of the Earth's crust and seismic activity: the example of Southern California, *Dokl., Earth Sci.,* 2010, vol. 430, no. 1, pp. 147–150. https://doi.org/10.1134/S1028334X10010320

Bondur, V.G., Aerospace methods and technologies for monitoring oil and gas areas and facilities, *Izv., Atmos. Oceanic Phys.,* 2011, vol. 47, no. 9, pp. 1007–1018. https://doi.org/10.1134/S0001433811090039

Bondur, V.G., Krapivin, V.F., Potapov, I.I., and Soldatov, V.Ju., Natural disasters and the environment, *Probl. Okr. Sredy Prir. Resur.,* 2012, no. 1, pp. 3–160.

Bondur, V.G., Garagash, I.A., and Gokhberg, M.B., Large scale interaction of seismically active tectonic provinces: the example of Southern California, *Dokl., Earth Sci.,* 2016a, vol. 466, no. 2, pp. 183–186. . https://doi.org/10.1134/S1028334X16020100

Bondur, V.G., Garagash, I.A., Gokhberg, M.B., and Rodkin, M.V., The evolution of the stress state in Southern California based on the geomechanical model and current seismicity, *Izv., Phys. Solid Earth,* 2016b, vol. 52, no. 1, pp. 117–128. https://doi.org/10.1134/S1069351316010043

Bondur, V.G., Chimitdorzhiev, T.N., Dmitriev, A.V., Dagurov, P.N., Zakharov, A.I., and Zakharova, L.N., Application of radar polarimetry to monitor changes in backscattering mechanisms in landslide zones using the example of the collapse of the Bureya River bank, *Izv., Atmos. Oceanic Phys.*, 2020, vol. 56, no. 9, pp. 916–926. https://doi.org/10.1134/S0001433820090054

Bondur, V.G., Chimitdorzhiev, T.N., Dmitriev, A.V., and Dagurov, P.N., Spatial anisotropy assessment of the forest vegetation heterogeneity at different azimuth angles of radar polarimetric sensing, *Izv., Atmos. Oceanic Phys.*, 2019, vol. 55, no. 9, pp. 926–934. https://doi.org/10.1134/S0001433819090093

Chimitdorzhiev, T.N. Zakharov, A.I., Tat'kov, G.I., Khaptanov, V.B., Dmitriev, A.V., Budaev, R.Ts., and Tsybenov, Yu.B., Study of soils cryogenic deformation in Selenga River delta by means of SAR interferometry and georadar sounding, *Issled. Zemli Kosmosa,* 2011, no. 5, pp. 58–63.

Colesanti, C. and Wasowski, J., Investigating landslides with spaceborne synthetic aperture radar (SAR) interferometry, *Eng. Geol.,* 2006, vol. 88, pp. 173–199.

Epov, M.I., Mironov, V.L., Chymitdorzhiev, T.N., Zakharov, A.I., Zakharova, L.N., Seleznev, V.S., Emanov, A.F., Emanov, A.A., and Fateev, A.V., Observation of Earth's surface subsidence in the area of Kuzbas underground coal mining with ALOS PALSAR radar interferometry, *Issled. Zemli Kosmosa,* 2012, no. 4, pp. 26–29.

Ferretti, A., Prati, C., and Rocca, F., Nonlinear subsidence rate estimation using permanent scatterers in differential SAR interferometry, *IEEE Trans. Geosci. Remote Sens.,* 2000, vol. 38, no. 5, pp. 2202–2212.

Ferretti, A., Fumagalli, A., Novali, F., Prati, C., Rocca, F., and Rucci, A., A new algorithm for processing interferometric data-stacks: SqueeSAR, *IEEE Trans. Geosci. Remote Sens.,* 2011, vol. 49, no. 9, pp. 3460–3470.

Hooper, A., Segall, P., and Zebker, H., Persistent scatterer interferometric synthetic aperture radar for crustal deformation analysis, with application to Volcan Alcedo, Galapagos, *J. Geophys. Res.: Solid Earth,* 2007, vol. 112, no. B7, pp. B07407-1–B07407-21.

Kimura, H. and Yamaguchi, Y., Detection of landslide areas using satellite radar interferometry, *Photogramm. Eng. Remote Sens.,* 2000, vol. 66, pp. 337–344.

Korenyuk, I.Yu., *Zhivaya Bureya* (Alive Bureya), Khabarovsk, RusGidro, 2009.

Kramareva, L.S., Lupyan, E.A., Amel'chenko, Yu.A., Burtsev, M.A., Krasheninnikova, Yu.S., Sukhanova, V.V., and Shamilova, Yu.A., Observation of the hill collapse zone near the Bureya River on December 11, 2018, *Sovr. Probl. Dist. Zond. Zemli Kosmosa,* 2018, vol. 15, no. 7, pp. 266–271.

Kramareva, L.S., Lupyan, E.A., Amel'chenko, Yu.A., Burtsev, M.A., Krasheninnikova, Yu.S., Sukhanova, V.V., Shamilova, Yu.A., and Boroditskaya, A.V., Observing the progress of blasting operations and channeling in the area of the rock slide on the Bureya River, *Sovr. Probl. Dist. Zond. Zemli Kosmosa,* 2019, vol. 16, no. 1, pp. 259–265.

Opolzen na r. Bureya (Landslide on Bureya River). http://omdoki.nextgis.com/resource/103/display (Accessed on July 1, 2019).

Ostroukhov, A.V., Kim, V.I., and Makhinov, A.N., Estimation of the morphometric parameters of the landslide on the Bureya reservoir and its consequences on the basis of remote sensing data and field measurements, *Sovr. Probl. Dist. Zond. Zemli Kosm.,* 2019, vol. 16, no. 1, pp. 254–258.

Prirodnye opasnosti Rossii (Natural Hazards of Russia), vol. 2. *Seismicheskie opasnosti* (Seismic Hazards) Sobolev, G.A., Ed., Moscow: KRUK, 2000.

Strozzi, T., Wegmuller, U., Werner, C., Wiesmann, A., and Spreckels, V., JERS SAR interferometry for land subsidence monitoring, *IEEE Trans. Geosci. Remote Sens.,* 2003, no. 41, pp. 1702–1708.

Strozzi, T., Teatini, P., Tosi, L., Wegmuller, U., and Werner, C., Land subsidence of natural transitional environments by satellite radar interferometry on artificial reflectors, *J. Geophys. Res.: Earth Surface,* 2013, vol. 118, pp. 1177–1191.

Xia, Y., Kaufmann, H., and Guo, X.F., Landslide monitoring in the Three Gorges area using D-INSAR and corner reflectors, *Photogramm. Eng. Remote Sens.,* 2004, no. 70 (10), pp. 1167–1172.

Zakharov, A.I. and Zakharova, L.N., Observation of snow cover dynamics on L-band SAR interferograms, *Sovr. Probl. Dist. Zond. Zemli Kosm.,* 2017, vol. 14, no. 7, pp. 190–197.

Zakharova, L.N. and Zakharov, A.I., Interferometric observation of landslide area dynamics on the Bureya river by means of Sentinel-L radar data in 2017–2018, *Sovr. Probl. Dist. Zond. Zemli Kosm.,* 2019, vol. 16, no. 2, pp. 273–277.

Zakharova, L.N., Zakharov, A.I., and Mitnik, L.M., First results of the assessment of the landslide consequences on the Bureya River bank using Sentinel-1 radar data, *Sovr. Probl. Dist. Zond. Zemli Kosm.,* 2019, vol. 16, no. 2, pp. 69–74.

Translated by E. Morozov